archives
of thermodynamics
Vol. **37**(2016), No. 4, 121–135
DOI: 10.1515/aoter-2016-0031

Study on transport packages used for food freshness preservation based on thermal analysis

YING YU*

Hunan Vocational College of Railway Technology, 171, Jianshe Middle Road, Zhuzhou, Hunan, 412000, China

Abstract In recent time, as the Chinese consumption level increases, the consumption quantity of high-value fruits, vegetables and seafood products have been increasing year by year. As a consequence, the traffic volume of refrigerated products also increases yearly and the popularization degree of the cold-chain transportation enhances. A low-temperature environment should be guaranteed during transportation, thus there is about 40% of diesel oil should be consumed by the refrigerating system and the cold-chain transportation becomes very costly. This study aimed to explore methods that could reduce the cost of transport packages of refrigerated products. On the basis of the heat transfer theory and the fluid mechanics theory, the heat exchanging process of corrugated cases during the operation of refrigerating system was analyzed, the heat transfer process of corrugated cases and refrigerator van was theoretically analyzed and the heat balance equation of corrugated cases was constructed.

Keywords: Heat transfer theory; Logistics transportation; Ansys Flotran; Temperature distribution

1 Introduction

China is a country with a large production of agricultural products, where the trade volume of agricultural products in China is increasing gradually year by year. Fresh food takes a great proportion of demand in market; however, due to the neglect of transport caused by excessive emphasis on

*E-mail: yingyu23y@sina.com

production, the development of fresh food transport is limited severely [1–3]. Continually increasing consumption of high-value fruits, vegetables and seafood products has resulted in the increase of traffic volume of refrigerated products. The increase of cold-chain demand has been particularly outstanding in the fields of meet products, fruits and vegetables, dairy products and medicine [4–6]. Temperature control of products is the key parameter during the whole process of cold-chain transportation and any phenomenon of out-of-control temperature can lead to enormous losses [7–9]. Thus, the temperature should be controlled precisely to guarantee the quality of products during transportation. Therefore, changes and field distribution of temperatures of the interior carriage and packing cases of products during transportation should be analyzed. The final results have great guidance values to the design of transport packages of products.

Lots of research results of the temperature field of refrigerated products have been obtained in other countries. Initial researches were mostly performed by experiments. Researchers in country-region Italy once carried out experiments based on the railway, and various kinds of standardizing components were used to simulate product models, thus to analyze the temperature distribution of interior packages. As the computer technology develops rapidly at present, the temperature filed has been studied using numerical simulation. Quarini and Foster studied the heat exchange between the cold air of freezer and the outside, and the obtained results were of great value to the design of energy-efficient refrigerators. In this study the commercial Ansys Flotran software was used to simulate temperature changes of products inside the refrigerator van, and the temperature field and temperature changes of the whole van were obtained. At last, obtained results were concluded, and improved cryogenic temperature and refrigerating method that could reduce energy consumption and save costs were planned, thus to obtain the optimal transportation program.

2 Model of phase change heat transfer

2.1 Basic theories of heat transfer theory

Fourier law is a fundamental law of heat transfer theory [10–12], which can be described as follow: in phenomena of heat conduction, suppose the heat quantity that passes through the interface in unit time is in direct proportion to the change rate of temperature in vertical direction of the interface as well as to the area of the interface, then the direction of heat transfer

is contrary to the direction of the temperature increase [13]. According to the Fourier law, the quantity of heat conduction, Φ, that passes through one position in unit time should be in direct proportion to the change rate of temperature as well as the area of the position:

$$\Phi = -\lambda A \frac{dt}{dx} = \lambda A \frac{\Delta t}{\delta} \,, \tag{1}$$

hence the heat flux that transfers along the x direction is

$$q = \frac{\Phi}{A} = \lambda \frac{\Delta t}{\delta} \,. \tag{2}$$

In above equations Φ refers to the rate of heat, λ refers to the thermal conductivity coefficient, t means temperature, x is the coordinate on heat conduction surface, A is heat conduction area, Δt is the temperature difference of surface, and dt/dx is the temperature gradient in the direction of x, i.e., the change rate of temperature (the negative sign in Eq.(1) means that, the heat transfer direction is contrary to the direction of the temperature gradient), δ is the thickness of surface.

3 Thermal analysis

Using the finite element software for numerical thermal analysis is to apply the principle of conservation of energy to construct the heat balance equation and obtain the temperature of each node through finite element calculation; other thermal physics parameters of the material can be educed according to temperatures of nodes. Steady-state analysis and transient analysis can be performed.

3.1 Thermal analysis governing equation

The governing differential equation of heat conduction:

$$\frac{\partial}{\partial x}\left(k_{xx}\frac{\partial T}{\partial x}\right) + \frac{\partial}{\partial y}\left(k_{yy}\frac{\partial T}{\partial y}\right) + \frac{\partial}{\partial z}\left(k_{zz}\frac{\partial T}{\partial z}\right) + q = \rho c \frac{dT}{dt} \,, \tag{3}$$

$$\frac{dT}{dt} = \frac{\partial T}{\partial t} + V_x\frac{\partial T}{\partial x} + V_y\frac{\partial T}{\partial y} + V_z\frac{\partial T}{\partial z} \,, \tag{4}$$

where T is the temperature, q is the heat flux, ρ is the density, c is the specific heat, k_{xx}, k_{yy}, k_{zz} and, V_x, V_y, V_z refer to velocity components

in x, y, z directions respectively and conduction rates, respectively x, y, z, are the Cartesian coordinates, and t denotes time. Equation (3) can be transformed into equivalent integral form

$$\int_{vol}\left[\rho c\delta_T\left(\frac{\partial T}{\partial t}+\{v\}^\top\{L\}^\top\right)+\{L\}^\top\delta_T\left(\{D\}\{L\}^\top\right)\right]d(vol)= \\ =\int_{S_2}\delta_T q^* d(S_2)+\int_{S_3}\delta_T h_f(T_B-T)\,d(S_3)+\int_{vol}\delta_T q d(vol)\ , \quad (5)$$

where vol refers to the element volume, $\{L\}^\top=\left[\frac{\partial}{\partial x}\frac{\partial}{\partial y}\frac{\partial}{\partial z}\right]$, q is the heat generation of unit volume, h_f refers to convective heat transfer coefficient, T_B is the temperature of fluid, δ_T is the dummy variable of temperature, S_2 and S_3 are the application areas of heat flux and convection, respectively, superscript $^\top$ denotes transpose operation.

Polynomial of unknown temperatures can be written as

$$T=\{N\}^\top\{T_e\}\ , \quad (6)$$

where $\{T_e\}$ refers to temperature vectors of element nodes and $\{N\}^T$ is the shape function of element.

Heat flux and temperature gradient of each element can be calculated according to temperatures of element nodes

$$\{a\}=\{L\}^\top=[B]\{T_e\}\ , \quad (7)$$

where $\{a\}$ refers to the thermal gradient vector and $[B]=\{L\}^T[N]$.

Heat flux can be calculated according to equation

$$\{q\}=(D)\{L\}^\top=(D)[B]\{T_e\}=(D)\{a\}\ , \quad (8)$$

where (D) refers to the property matrix of heat conduction of the material.

$$\int_{vol}\rho c\{N\}^\top\{N\}d(vol)\{T_e\}+\int_{vol}\rho c\{N\}^\top\{v\}^\top[B]d(vol)\{T_e\} \\ +\int_{vol}(B)^\top(D)(B)d(vol)\{T_e\}=\int_{S_2}\{N\}q^* d(S_2)+\int_{S_2}T_B h_f\{N\}d(S_3) \\ -\int_{S_2}h_j\{N\}^\top\{N\}\{T_e\}d(S_3)+\int_{vol}q(vol)\ . \quad (9)$$

Matrix form of the above equation is

$$(C)\{T\} + ((K^m) + (K^d) + (K^c))\{T\} = (Q^f) + (Q^c) + (Q^g) \,, \tag{10}$$

where:

$$(K^m) = \int\limits_{vol} \rho c \{N\}^T \{v\}^T [B] \, d(vol) \,,$$

$$(K^d) = \int\limits_{vol} (B)^T (D) (B) \, d(vol) \,,$$

$$(K^c) = \int\limits_{s_2} h_f \{N\}^T \{N\} \, d(S_3) \,,$$

$$(Q^f) = \int\limits_{s_2} \{N\} q^* d(S_2) \,,$$

$$(Q^c) = \int\limits_{S_2} T_B h_f \{N\} \, d(S_3) \,,$$

$$(Q^g) = \int\limits_{vol} q d(vol) \,,$$

The general equation matrix can be expressed as

$$(C)\{T\} + (K)\{T\} = \{Q\} \,, \tag{11}$$

where:

$$(C) = \sum_{i=1}^{n} (C)_i \,,$$

$$(K) = \sum_{i=1}^{n} (K^{m,d,c})_i \,,$$

$$(Q) = \sum_{i=1}^{n} \{Q^{f,c,g}\}_i + \{Q_0\} \,,$$

here n refers to the number of elements and $\{Q_0\}$ refers to the rate of heat flow applied to nodes.

3.2 Processing of phase change problems using the finite element software

A kind of large scale and general finite element analysis software – that integrates electric field, magnetic field, sound field, structure, load, temperature field and fluid analysis – Ansys [14–16] has been used.

The used finite element analysis software considers the latent heat of phase-change materials through defining their enthalpy value, which changes along with the change of temperature. Changes of enthalpy value can be described by the function expression of density, ρ, specific heat C and temperature, T:

$$\Delta H = \int \rho C(T) dT \ . \tag{12}$$

Internal and external heat quantity of composite corrugated cases of fruits packaging system includes three parts:

external high-temperature air transfers heat to the inside of boxes through the box wall – q_1,

heat brought by the gas exchange between side wall gaps of boxes inside the system – q_2,

respiratory heat produced by fruits – q_3.

The total heat, Q_1, produced by above three methods after h hours is

$$Q_1 = h(q_1 + q_2 + q_3) = h\Big[KA(T_1 - T_2 + M(i_i - i_2) + 2.553\,Gu\Big] \ , \tag{13}$$

where K refers to the heat transfer coefficient of the whole box, T_1 and T_2 are the internal and external temperatures of the box, respectively, A is the superficial area of the box, M is the quantity of heat exchange air every hour, G is the mass of fruits, i_1 and i_2 are specific enthalpy of the internal and external air of the box, respectively, u is the quantity of CO_2 produced by respiration of fruits in 1 h.

Suppose the freshness of fruits can be preserved for h hours at temperature $T\,^{\circ}$C, meaning that the color, aroma, taste and edible value of fruit are not affected. The endothermic process of fruits in the box is also a constant-pressure process, thus the heat consumed by increase of 1 °C of fruits is constant-pressure specific heat, C_p. The symbol Q_2 refers to the quantity of heat consumed by the increase of fruits temperature from T_1 to T. Suppose other heat losses are ignored, then according to the law of

conservation of energy, the total heat, Q_1, input by external environment is equal to the heat, Q_2, absorbed by fruits

$$Q_1 = Q_2 = GC_p(T - T_1) \ . \tag{14}$$

Heat-shielding performance of composite corrugated cases was simulated in this study. Heated pure water (physical heat source) was used to replace the respiratory heat of fruits (biological heat source). Thus, according to Eqs. (13) and (14):

$$Q_1 = h\big[KA(T_1 - T_2) + M(i_1 - i_2)\big] = cM_1(T - T_1) \ , \tag{15}$$

where c refers to the specific heat of water and M_1 is the mass of heated pure water. Specific enthalphy of internal air and external air of the box is $i_1 - i_2 = (1.01 + 1.84d)(T_1 - T_2)$, where d denotes the relative humidity of air. Thus the computational formula of heat conductivity coefficient, K, of the whole box can be obtained from Eq. (15)

$$K = \frac{cM_1(T - T_1)}{hA(T_1 - T_2)} - \frac{M(1.01 + 1.84d)}{A} \ . \tag{16}$$

4 Heat balance of refrigerator van

A mechanical refrigerated car used for short-distance refrigerated transport was taken as the research object in this study. The size of the car was, length×width×height, of 4.2 m × 2.2 m × 2.2 m. Polyurethane extruded sheet was used as the thermal insulation material of the car and its thickness was 0.1 m. The refrigerating system was inside the car, which could adjust the temperature.

4.1 Heat balance method

Heat balance method refers to considering all kinds of factors of dissipation of cooling capacity of the refrigerator car on the basis of the heat balance theory, and such method has accurate calculation, while it is also complicated in calculation of the thermal load of refrigerator. The total thermal load of the refrigerator car is the sum of load from outside and the load produced inside the car, which includes following four parts:

$$Q = Q_1 + Q_2 + Q_3 + Q_4 \ . \tag{17}$$

1. Heat, Q_1, introduced from the outside environment can be expressed as

$$Q_1 = 1.1(Q_b + Q_s + Q_l + Q_d) \,, \tag{18}$$

where factor 1.1 refers to the loss coefficient. Q_b is the heat quantity introduced through the car (W),

$$Q_b = KF_m(t_e - t_i) \,, \tag{19}$$

where K refers to the overall heat transfer coefficient of the car, and

$$F_m = \sqrt{F_e F_i} \,, \tag{20}$$

is the average heat transfer area of the car, where F_e and F_i are the exterior and interior superficial area of the car, respectively. In Eq. (19) t_e refers to the average temperature of environment and t_i is the average temperature inside the car). Q_s refers to the heat quantity transferred into the car from solar radiation,

$$Q_s = KF_s\Delta t_s\frac{\tau_s}{24} \,, \tag{21}$$

where F_s refers to the area affected by solar radiation, Δt_s is the increase of temperature under the effect of solar radiation, and τ_s is the time of solar radiation. Q_l refers to heat quantity introduced by air permeation,

$$Q_l = \beta\, Q_b \,, \tag{22}$$

where β is the additional heat load coefficient of air permeation. Q_d refers to heat quantity introduced by the open of car door,

$$Q_d = f\,(Q_b + Q_s) \,, \tag{23}$$

where f is the additional heat load coefficient of door opening (Tab. 1 shows the additional heat load coefficient of door opening during transportation).

2. Cooling capacity, Q_2, consumed by the thermal insulation material and the precooling of components is

$$Q_2 = \frac{1}{2}\sum(G\,C)\frac{\Delta t}{\Delta\tau} \,, \tag{24}$$

where G refers to the quality of thermal insulation materials or car components, C refers to corresponding specific heat, Δt is the temperature difference, and $\Delta\tau$ is the time difference.

Table 1: Additional heat load coefficient of door opening.

Opening frequency (times)	Additional heat load coefficient f
0	0.25
1-5	0.5
6-10	0.75
11-15	1

3. The cooling capacity, Q_3, consumed by the precooling of products is

$$Q_3 = G_f \, C_f \frac{\Delta t}{\Delta \tau} \, , \tag{25}$$

where G_f refers to the quality of products, and C_f is the specific heat of products.

4. Heat quantity, Q_4, produced inside the car is

$$Q_4 = Q_f + Q_i \, . \tag{26}$$

Here

$$Q_f = G_f q_f \tag{27}$$

refers to the heat release of products (respiratory heat of vegetables, etc.), where q_f is the heat released by products per kilogram per hour, and

$$Q_i = P_i t_i \frac{1}{24} \tag{28}$$

refers to heat quantity produced by illumination inside the car, where P_i is the power of lighting, and t_i is the illuminating period.

During the transportation of the eutectic plate refrigerated car, the cooling consumption amount is balanced by melting of eutectic ice, thus to maintain the low temperature inside the car and guarantee the quality of fresh products.

4.2 Stacking of refrigerated products inside the car

Spaces between products and products and the car wall should be guaranteed because good heat exchange and temperature require good ventilation.

Figure 1 shows a way of stacking products; A1 refers to the car body and A2, . . . , A9 refers to the stacking area. Each stacking area has a push plate. Each push plate is placed with three layers of products and each layer is placed with two packing boxes. The space between car roof and the top of third layer is 0.1 m, the distance between boxes and car wall is 0.15 m, the distance between A2 and A6 and the car tail is 0.2 m, the distance between A5 and A9 and front of car is 0.3 m, the line spacing and row spacing are 0.1 m and 0.2 m, respectively [17].

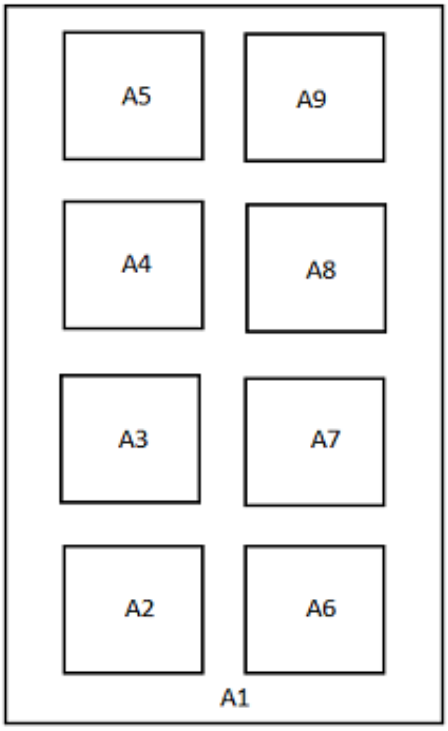

Figure 1: Stacking of products.

5 Heat produced by car during the process of transportation

Heat produced by the refrigerator car during transportation can be divided into two kinds: heat produced by quality degradation of thermal insulation

materials of car or door opening during transportation

$$Q_1 = \lambda_0 S \Delta T \,, \tag{29}$$

and heat caused by thermal radiation of the sun

$$Q_2 = 0.45 \lambda_0 S \Delta T^{'} Z \,. \tag{30}$$

In above equations λ_0 refers to the heat conductivity of the car, which is 0.55 W/(m K), S is the the heat exchange area of car, ΔT and $\Delta T^{'}$ are the temperature difference inside and outside the car, and between car surface and the inside of car, respectively, Z is environmental coefficient.

6 Simulation of temperature field inside the refrigerator car

Using Ansys Flotran software, this study simulated and analyzed the temperature field inside the refrigerator car [18,19].

6.1 Modeling and grid generation

Construction of models is accomplished by the modeling module of Ansys software. The top view of car is drawn by using Solid 8node77 for grid generation. Stocking areas A2, A3, A4, A5, A6, A7, and A8 are spaces for corrugated boxes. Gas flow space of the car and the overall space of the car are given grid generation [20–22].

6.2 Definition of material parameters

Parameters of products [23] Bergamot pears were used as the research objects in this study, because they had regular shapes, thus spaces between pears could be left after pears were placed in boxes, which made the simulation results much closer to the reality. The shape of bergamot pears was taken as a sphere approximately in this study and the diameter was $D = 0.6$ m; the heat conductivity of the bergamot pear was $\lambda = 0.14$ W/(m K.

Suppose bergamot pears occupied 60% of the volume in each corrugated box, porosity $\zeta = 0.4$, density of bergamot pears is $\rho = 700$ kg/m^3 and the specific heat capacity of bergamot pears $C = 2.45$ KJ/(kg K). Appropriate temperature for transportation of bergamot pears is 5 °C.

Physical property parameters of the cold air in car Power of the refrigeration equipment was 1050 W when the operating temperature was 0 °C, when the operating temperature exceeded 3 °C the power was 900 W. Air density $\rho = 1.228$ kg/m^3; heat conductivity of air was $\lambda = 0.16$ W/(m K); coefficient of thermal expansion of air was $\beta = 3.378 \times 10^{-3}$ 1/K, dynamic coefficient of viscosity of air was $\mu = 1.85 \times 10^{-5}$ N s/m^2, specific heat capacity of air was $C = 2.62$ KJ/(kg K); air speed of cold air outlet was $v = 1$ (m/s), temperature of cold air was $t = 0.3$ °C.

6.3 Results of simulation and analysis

Average temperatures of products in the car at different cryogenic temperatures are shown in Fig. 2.

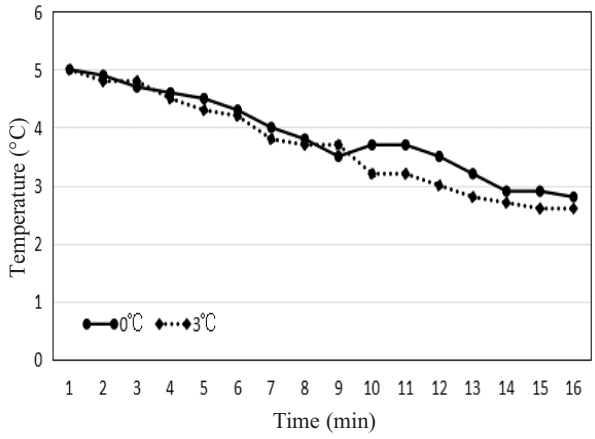

Figure 2: Average values of temperature changes of products.

Figure shows that, the temperature changes of products during transportation are nonlinear. The total distance covered by the refrigerator car was 120 km, which takes 3 h; during the transportation, different temperatures inside of car could lead to different consumption of energy. Specific data are shown in Tab. 2.

Data in table show that, in the first kind of refrigerating method, the refrigerating temperature was 0 °C and the refrigerating time was 15 min for each time, 20 min of pause between each time, thus the overall operating time of the refrigerating system was 60 min and energy consumption was

Table 2: Energy consumption in different refrigerating methods.

Refrigerating temperature (°C)	0	3
Number of refrigerations	4	5
Energy consumption (KJ)	3.75×10^3	2.74×10^3

3.75×10^3 KJ. In the second kind of refrigerating method, the refrigerating temperature was 3 °C and the refrigerating time was 10 min for each time, 15 min of pause between each time, thus the overall operating time of the refrigerating system was 50 min and the energy consumption was 2.74×10^3 KJ. Obviously, the second method not only satisfied the low-temperature operation, but also saved 1.01×10^3 KJ of energy consumption, which decreased by 26.9% and reduced transportation costs. Thus the second method was more appropriate for refrigeration.

7 Summary

This study analyzes heat balance of corrugated boxes based on elementary knowledge of heat transfer theory, and the heat balance equation of corrugated boxes is constructed on the basis of heat transfer process of corrugated boxes, heat exchange of ventilation hole, and respiratory heat of products. Some of the minor parameters are neglected in the thermal analysis of products, such as the self respiration heat of different fruits and vegetables, thus this study has certain limitations.

Received 28 May 2016

References

[1] Zhang Z., Gao Z., Min L.I. *et al.*: *Effect of food additives on postharvest pathogens and preservation of mango fruit*. Chinese J. Tropical Crops **34**(2013), 11, 2289–2294.

[2] Zhang B.N., Zhu X.Y., Lai J.: *Effect of ozone water treatment on preservation of chinese chestnut fruits during storage*. Food Sci. **32**(2011), 16, 361–364.

[3] Wang F.C., Jun-Guo L.I., Dong Y.C. *et al.*: *Research progress of application of polysaccharides and modified polysaccharides in film coatings for food preservation*. Food Sci. **33**(2012), 5, 299–304.

[4] Tan Y.B., Zhang Q.Y.: *Food cold chain transportation management based on grid technology*. Appl. Mech. Mater. **543-547**(2014), 4540–4542.

[5] Jia K.: *Design of wireless sensor node in cold chain transportation monitoring.* Trans. Chinese Soc. Agricultural Machinery **44**(2013), 2, 136–141.

[6] Net M., Trias E., Navarro A. *et al.*: *Cold chain monitoring during cold transportation of human corneas for transplantation.* Transpl. P. **35**(2003), 5, 2036–2038.

[7] Yue J., Liu L., Li Z. *et al.*: *Improved quality analytical models for aquatic products at the transportation in the cold chain.* Math. Comput. Model. **58**(2013), 3–4, 474–479.

[8] Liu L., Hu J.y., Zhang J.j. *et al.*: *Development of time-temperature data collection program for frozen fish in the cold chain.* Sensor Lett. **8**(2010), 1, 47–51.

[9] Jedermann R., Ruiz-Garcia L., Lang W.: *Spatial temperature profiling by semi-passive RFID loggers for perishable food transportation.* Comput. Electron. Agr. **65**(2009), 2, 145–154.

[10] Jaremkiewicz M.: *Determination of transient fluid temperature using the inverse method.* Arch. Thermodyn. **35**(2014), 1, 61–76.

[11] Mikielewicz D., Andrzejczyk R., Jakubowska B. *et al.*: *Comparative study of heat transfer and pressure drop during flow boiling and flow condensation in minichannels.* Arch. Thermodyn. **35**(2014), 3, 17–37.

[12] Vasiliev L., Vasiliev L., Zhuravlyov A. *et al.: Vapordynamic thermosyphon - heat transfer two-phase device for wide applications.* Arch. Thermodyn. **36**(2015), 4, 65–76.

[13] Mikielewicz D., Muszyński T., Mikielewicz J.: *Model of heat transfer in the stagnation point of rapidly evaporating microjet.* Arch. Thermodyn. **33**(2012), 1, 139–152.

[14] Wang J.L.: *Based on the finite element software ANSYS/LS-DYNA metal plate covering parts forming process simulation and optimization research.* Adv. Mater. Res. **912–914**(2014),589–592.

[15] Oluwole L., Odunfa A.: *Investigating the effect of ocean waves on gravity based offshore platform using finite element analysis Software ANSYS.* Int. J. Sci. Eng. Res. **6**(2015), 8, 24–33.

[16] Delele M.A., Ngcobo M.E.K., Opara U.L. *et al.*: *Investigating the effects of table grape package components and stacking on airflow, heat and mass transfer using 3-D CFD modelling.* Food Bioprocess Tech. **6**(2013), 9, 2571–2585.

[17] Defraeye T., Verboven P., Opara U.L. *et al.*: *Feasibility of ambient loading of citrus fruit into refrigerated containers for cooling during marine transport.* Biosyst. Eng. **134**(2015), 20–30.

[18] Zhou Y.: *Effect of velocity of fluid field of 3-spacer nozzle in roll-casting models using coupled fluid-thermal finite element analysis.* Appl. Mech. Mater. **29-32**(2010), 1481–1487.

[19] Elnaggar M.H.A., Abdullah M,Z., Munusamy S.R.R.: *Experimental and numerical studies of finned L-shape heat pipe for notebook-PC cooling.* IEEE T. Comp. Pack. Man. **3**(2013), 6, 978–988.

[20] Mamun K.A., Stokes J.: *Development of a semi automated dual feed unit to produce FGM coatings using the HVOF thermal spray process.* South Pacific J. Natural Appl. Sci. **32**(2014), 1, 18–26.

[21] Luo Z.B.: *Effects of different vents location on flow characteristics of air conditioning.* Appl. Mech. Mater. **622** (2014), 179–182.

[22] Spano M., Stara V.: *Application of a 2D turbulence model for estimation of the discharge coefficient on round-shaped weirs.* AIP Conf. Proc. **1048**(2008), 1, 806–809.

[23] Xiao Y., Liu D.: *Agricultural products refrigerated and insulated transport technology and equipment research.* J. Agr. Mech. Res. **33**(2011), 1, 57–60.